Physics and Imaging in Radiation Oncology 9 (2019) 69–76

Contents lists available at ScienceDirect

Physics and Imaging in Radiation Oncology

journal homepage: www.elsevier.com/locate/phro

Original Research Article

Clinical implementation of magnetic resonance imaging guided adaptive radiotherapy for localized prostate cancer

Shyama U. Tetar, Anna M.E. Bruynzeel, Frank J. Lagerwaard, Ben J. Slotman, Omar Bohoudi, Miguel A. Palacios*

Dept. of Radiation Oncology, VU University Medical Center, de Boelelaan 1117, 1081 HV Amsterdam, The Netherlands

ARTICLE INFO

Keywords:
Prostate cancer
MR-guided Radiotherapy (MRgRT)
Stereotactic body radiotherapy (SBRT)
On-table adaptation
Workflow

ABSTRACT

Background and purpose: Magnetic resonance-guided radiation therapy (MRgRT) has recently become available in clinical practice and is expected to expand significantly in coming years. MRgRT offers marker-less continuous imaging during treatment delivery, use of small clinical target volume (CTV) to planning target volume (PTV) margins, and finally the option to perform daily plan re-optimization.

Materials and methods: A total of 140 patients (700 fractions) have been treated with MRgRT and online plan adaptation for localized prostate cancer since early 2016. Clinical workflow for MRgRT of prostate cancer consisted of patient selection, simulation on both MR- and computed tomography (CT) scan, inverse intensity-modulated radiotherapy (IMRT) treatment planning and daily plan re-optimization prior to treatment delivery with partial organs at risk (OAR) recontouring within the first 2 cm outside the PTV. For each adapted plan online patient-specific quality assurance (QA) was performed by means of a secondary Monte Carlo 3D dose calculation and gamma analysis comparison. Patient experiences with MRgRT were assessed using a patient-reported outcome questionnaire (PRO-Q) after the last fraction.

Results: In 97% of fractions, MRgRT was delivered using the online adapted plan. Intrafractional prostate drifts necessitated 2D-corrections during treatment in approximately 20% of fractions. The average duration of an uneventful fraction of MRgRT was 45 min. PRO-Q's (N = 89) showed that MRgRT was generally well tolerated, with disturbing noise sensations being most commonly reported.

Conclusions: MRgRT with daily online plan adaptation constitutes an innovative approach for delivering SBRT for prostate cancer and appears to be feasible, although necessitating extended timeslots and logistical challenges.

1. Introduction

External beam radiotherapy (EBRT) is the treatment of choice in approximately one third of patients with localized prostate cancer (cT1c-T3N0M0) and this proportion increases with higher age. When EBRT is selected as the treatment of choice, the guideline-recommended total radiation dose for localized prostate cancer is 78–80 Gy. However, delivering this total dose in small daily fractions (e.g. 1.8–2 Gy/fraction) requires up to eight weeks of fractionated EBRT. Prostate cancer appears to be characterized by a low α/β value and consequently, large radiation doses per fraction (hypofractionation) can be expected to increase tumour kill for prostate cancer while minimizing late toxicity to critical structures [1–3]. Based on this concept, many radiation oncology centers have adopted the concept of *moderate* hypofractionation (fraction sizes of 2.5–4 Gy) or *extreme* hypofractionation (fraction size > 4 Gy), also known as stereotactic body radiotherapy (SBRT) for routine treatment of localized prostate cancer.

Inter- and intra-fractional organ changes entail major problems for the safe delivery of intended doses in EBRT for tumours located in the abdominal and pelvic region, especially for hypofractionated schemes. Substantial variability in rectum and bladder filling has been observed in the past for patients treated for prostate cancer [4–6] and lower biochemical tumour control was reported for patients with larger rectum volumes at the time of the CT simulation [7], presumably because of geographic misses. Several studies have investigated inter-fractional prostate variability by means of repeated CT, kV or online CBCT (for a review on this topic, see [8]). Mean prostate displacements of up to 9 mm between fractions have been reported, with the largest deviation found in the anterior-posterior (AP) direction [8,9]. Seminal vesicles, which are included in the target volume for intermediate and

* Corresponding author at: VU Amsterdam University Medical Center, Postbox 7057, 1007 MB Amsterdam, The Netherlands.
E-mail address: m.palacios@vumc.nl (M.A. Palacios).

https://doi.org/10.1016/j.phro.2019.02.002
Received 16 August 2018; Received in revised form 13 February 2019; Accepted 19 February 2019

high risk disease patients, are subjected to even larger inter-fractional shifts than the prostate [10]. In addition, intra-fractional rotations and deformations of prostate and seminal vesicles because of variable rectal filling have been reported [11]. Proper management of such inter- and intra-fractional variations during radiotherapy delivery may allow treatment margin reduction to 3 mm [12].

Daily image-guided radiotherapy (IGRT) improves the precision and accuracy of treatment delivery for prostate cancer [10]. Standard IGRT repositioning protocols based on patient registration on the prostate are able to adequately correct for the dosimetric effects of inter-fractional variations in approximately two-thirds of the treatment fractions [13]. Current employed IGRT techniques, such as kV radiographs or cone-beam computed tomography (CBCT) are usually combined with implanted fiducial markers; however these lack detailed target and organ at risk (OARs) visualization. MR-guided radiation therapy (MRgRT) allows for superior visualization of the prostate, base of the seminal vesicles and adjacent OARs such as the rectum and bladder prior to- and during treatment delivery. This allows for treatment with small uncertainty margins and in combination with daily plan re-optimization may result in relevant reductions of doses to normal tissues [14,15]. In addition, in-room MR imaging renders implanted gold markers redundant, thereby avoiding an invasive procedure.

Several published papers have described the use of MRgRT [16–19] in the upper abdominal region, but reports on the use of MRgRT for prostate cancer have been rather of theoretical nature [8,20]. In this study we describe the first clinical implementation of a daily online adaptive MRgRT workflow for SBRT in prostate cancer. Superior soft-tissue visualization in combination with intra-fraction motion management allowed us to reduce PTV margins to 3 mm and deliver doses of 7.25 Gy per fraction. We report on the time needed for our MRgRT clinical workflow and the frequency of online corrections due to intra-fractional variations in the prostate position. Patient reported outcomes of MRgRT and results from patient-specific QA are also presented. Finally, we aim to illustrate potential pitfalls of MRgRT for prostate cancer.

2. Materials and methods

At the Amsterdam University medical center, location VUmc, clinical MRgRT has been performed since early 2016 using the MRIdian® system (ViewRay, Inc., Mountain View, CA). For localized prostate cancer, MRgRT has been delivered in 140 patients in 700 fractions between May 2016 and June 2018, initially with the tri-^{60}Co system (n = 130), currently with the MR-Linac (n = 10). The majority (n = 100) of patients have been treated within the context of a prospective phase II trial. The clinical results of this trial will become available in mid-2019.

2.1. First consultation

All patients treated with MRgRT for prostate cancer were previously discussed in a multidisciplinary tumor board. Clinical stage of patients with localized prostate cancer treated with MRgRT was T1-3b without severe urinary symptoms as measured by International Prostate Symptom Scoring (IPSS). Patients with prior local treatment, e.g. high intensity focused ultrasound (HIFU), brachytherapy, or cryotherapy were not considered candidates for SBRT with the exception of a transurethral resection of prostate (TURP) if performed more than two months prior to radiation. All patients were routinely checked for contra-indications for MRgRT, similar as for diagnostic MR scans.

2.2. Simulation

Every patient underwent a CT simulation scan with a slice thickness of 2 mm for dose calculation purposes, and a high-resolution (HR) MR scan (TR/TE: 3.37 ms/1.45 ms, FA: 60°) acquired at the MRIdian (0.35T) with 1.5 mm × 1.5 mm × 1.5 mm resolution prior to treatment. The maximum time span between both examinations was 30 min. MR scan acquisition is based on a balanced steady-state free precession technique (True FISP) providing T2/T1-weighted contrast. The anatomy around the prostate exhibits similar contrast as in T2-weighted sequences, which is recommended for target volume delineation for primary radiation therapy of localized prostate cancer [21]. MR acquisition in the pelvic region for treatment planning at the MRIdian took between 65 and 172 s, depending on the scan range and field of view (FOV). Flexible coils were used which were placed around the patient in the pelvic region.

Simulation and delivery was executed in supine position with the use of coils and head phones for noise reduction. Patient positioning was performed on an MR-compatible positioning board (Macromedics, Waddinxveen, The Netherlands), including foot, knee and arm support. The acquired CT (with dummy coils) was non-rigidly co-registered with the simulation MR, with the fusion centered on the area of interest, i.e. the prostate. When gas in rectum was variable between the CT and MR simulation, special care was taken to obtain a good agreement between the anatomies reflected in both scans after non-rigid registration, especially in the area of the CTV (prostate). Patients were instructed to empty their bladder two hours before treatment, followed by intake of 500 ml of water. No specific rectal preparations such as endorectal balloons or pre-treatment enemas were required.

2.3. Target definition and radiation dose fractionation

For MRgRT of prostate cancer, target definition was basically identical to other techniques delivering SBRT. Briefly, the clinical target volume (CTV) was delineated on the simulation MR-scan. For 'low risk' patients (cT1c-T2a, Gleason < 7 and PSA < 10 µg/L), the CTV consisted of the prostate gland. For 'high' and 'intermediate risk' patients [22], the base of the seminal vesicles was also included in the CTV. As a result of daily MR-based setup, low spatial distortion, online plan adaptation and real-time prostate monitoring during treatment, only a 3 mm CTV to PTV uniform margin was used for MRgRT. For baseline planning, relevant OAR, i.e. the bladder, rectum, urethra and femora were contoured on the MR-scan. A good discrimination between the posterior border of the prostate and the anterior rectal wall was obtained with current MR True FISP sequence. Although not standard in SBRT for prostate cancer, in an attempt to decrease acute and late urinary toxicity, integrated urethral sparing was used by generating an urethral $PTV_{urethra}$ with a margin of 2–3 mm around the delineated urethra (Fig. 1). Most patients were treated with 5 fractions of 7.25 Gy per fraction delivered on the prostate with a simultaneous integrated sparing (SIS) of the urethra with a dose of 32.5 Gy in 5 fractions (6.5 Gy per fraction). In some cases (n = 10) with tumour near the urethra, the SBRT was delivered in fractions of 7 Gy up to a total dose of 35 Gy without urethral sparing. The majority of OAR constraints were expressed in absolute volume (cc), which allows partial contour delineation during the adaptive workflow (see also below).

2.4. Online contour generation

At each fraction, online new contours were generated for prostate, OARs and structures needed for treatment planning. Firstly, the CTV was rigidly copied from the pre-treatment MR scan to the MR volumetric scan of the day and both scans were rigidly registered on the target. The CTV is then edited by the physician when needed, accounting for rotations and deformations of the prostate and/or seminal vesicles. After that, a new PTV (CTV + 3 mm) was automatically generated to account for delineation uncertainties, intra-fraction motion and random spatial distortions on the MR-scan (less than 1 mm in a 20 cm DSV). A second non-rigid registration of both MR-scans was thereafter performed and the deformation field map was also applied to the OAR contours to generate structures reflecting the anatomy-of-the-

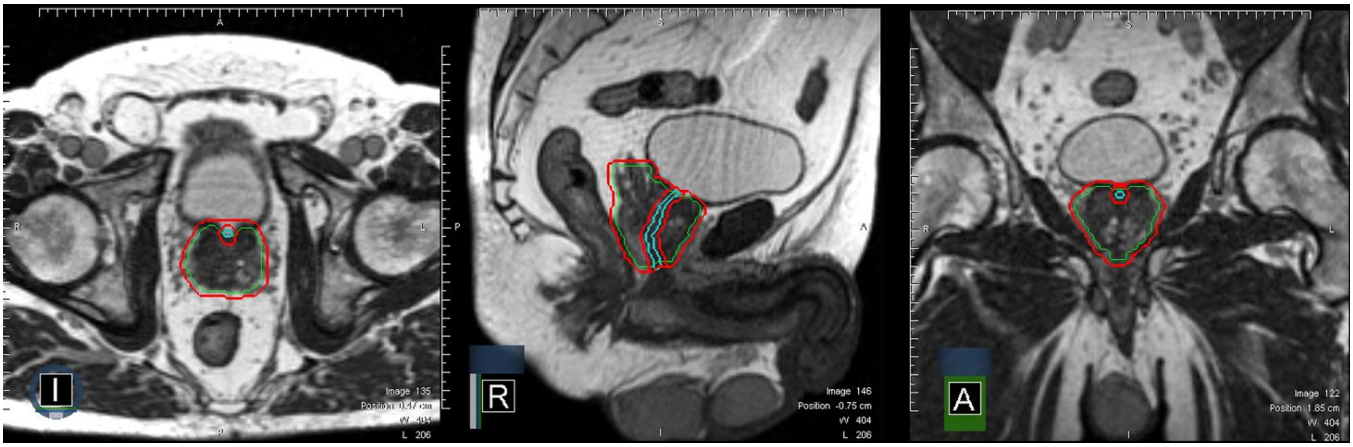

Fig. 1. Contouring for MRgRT: CTV consisting of prostate and base of vesicles (green contour), PTV (CTV + 3 mm; red contour) visualized in an axial, sagittal and coronal plane. The urethral contour (cyan contour) and urethral PRV (urethra + 2 mm) can be best seen in the sagittal plane. (For interpretation of the references to colour in this figure legend, the reader is referred to the web version of this article.)

day. The deformable registration algorithm implemented on the MRIdian and employed for online adaptive minimizes a cost function that measures the similarity between the images. It also uses a regularization term to obtain smoother deformation fields and prevents sharp discontinuities. The optimization method relies on a simple gradient descend performing the registration firstly on a down sampled version of the image serving the results as initial guesses for each upper level.

The electron density map generated from the CT for dose calculation underwent the same deformation applied to the OAR contours. The newly generated electron density map for that particular fraction was briefly checked by the radiation technologist and physicist for the presence of missing tissue densities and mismatch for air pockets in rectum. In case of mismatch, structure densities were overridden and corrected online before dose calculation and plan adaptation.

2.5. Treatment planning

Treatment planning and delivery was performed with static field intensity modulated radiotherapy (IMRT). A relatively high number of beams were used (15) which provided enough degrees of freedom and flexibility to re-adapt the plan and account for anatomical changes. Typically around 45 segments were generated which in combination with the different beam angle incidence produced treatment plans achieving the modulation needed for selective urethral sparing. The MRIdian Linac version uses a double focused, double-stacked multileaf collimation (MLC) in combination with 6MV FFF photons, allowing for highly conformal dose distributions and steep dose gradients at the borders with adjacent OARs. The obtained dosimetry for treatment planning in MRgRT is comparable to VMAT techniques [23]. Our treatment planning approach for MRgRT has been developed with daily plan adaptation in mind [24], and will be presented below.

Dose calculation was performed with a Monte-Carlo algorithm implemented in the MRIdian system based on VMC and EGSnrc codes [25,26]. The algorithm can complete an IMRT plan calculation subject to a magnetic field in 2 min. For clinical plans, a statistical uncertainty of 1% was used with a dose grid resolution of 0.2 cm × 0.2 cm × 0.2 cm.

2.6. MR-guided online adaptive workflow

A summary of the treatment workflow for MRgRT with daily plan adaptation implemented at our center is visualized in Fig. 2. After MR acquisition and patient registration, CTV and OAR contours always needed to be online adjusted by the attending radiation oncologist to correct for variations in the position of the upper part of the prostate and base of the seminal vesicles. For the daily plan adaptation whilst the patient is in treatment position, only OARs in the first 2 cm outside the PTV were corrected to allow for a fast online workflow.

At each fraction a new electron density map for dose calculation was generated after applying deformable image registration. Subsequently, two plans were generated: the baseline plan re-calculated on the anatomy-of-the-day (predicted plan) and the re-optimized plan. The re-optimized plan was generated by OAR partitioning within the first 2 cm from the PTV surface and updating all necessary structures for treatment planning by means of an automated script. Both plans were reviewed by the radiation oncologist and physicist whether they met the preset plan objectives. An example of the potential of plan adaptation in one patient undergoing an MRgRT treatment can be seen in Fig. 3, where the baseline plan, predicted plan and re-optimized plan for a particular fraction can be observed. Initial anatomy at baseline showed some distance between the prostate and rectum allowing for adequate coverage of CTV and sparing of rectum. However, rectum distension brought forth a pitch and deformation on the prostate at one particular fraction, resulting in suboptimal CTV coverage and an increased dose to the rectum. Online plan re-optimization following proposed strategy resulted in adequate rectum sparing and recovery of CTV coverage.

2.7. Patient-specific QA

Prior to plan approval at the treatment console, patient-specific quality assurance (QA) of the adapted plan was performed using an independent Monte-Carlo dose calculation algorithm and gamma analysis (3%/3 mm) [27–30]. The Monte-Carlo engine for QA purposes uses phase space data recorded in a plane just above the MLC and the transport in the patient is loosely based on the DPM Monte-Carlo code [31]. It used the same beam parameters, segments shapes and electron density map as the treatment plan made with the MRIdian, resulting in a second 3D dose distribution. At each fraction a pdf-report was generated including gamma pass-rates and gamma mean values for the comparison of both dose distributions. In addition, other plan parameters related to the IMRT modulation in the plan were also reported [27].

2.8. Patient reported questionnaires

From the start of clinical MRgRT, patient experiences were assessed using an in-house developed patient-reported outcome questionnaire (PRO-Q) [32]. From July 2016 till December 2017 we collected 89 questionnaires in prostate cancer patients. This PRO-Q included

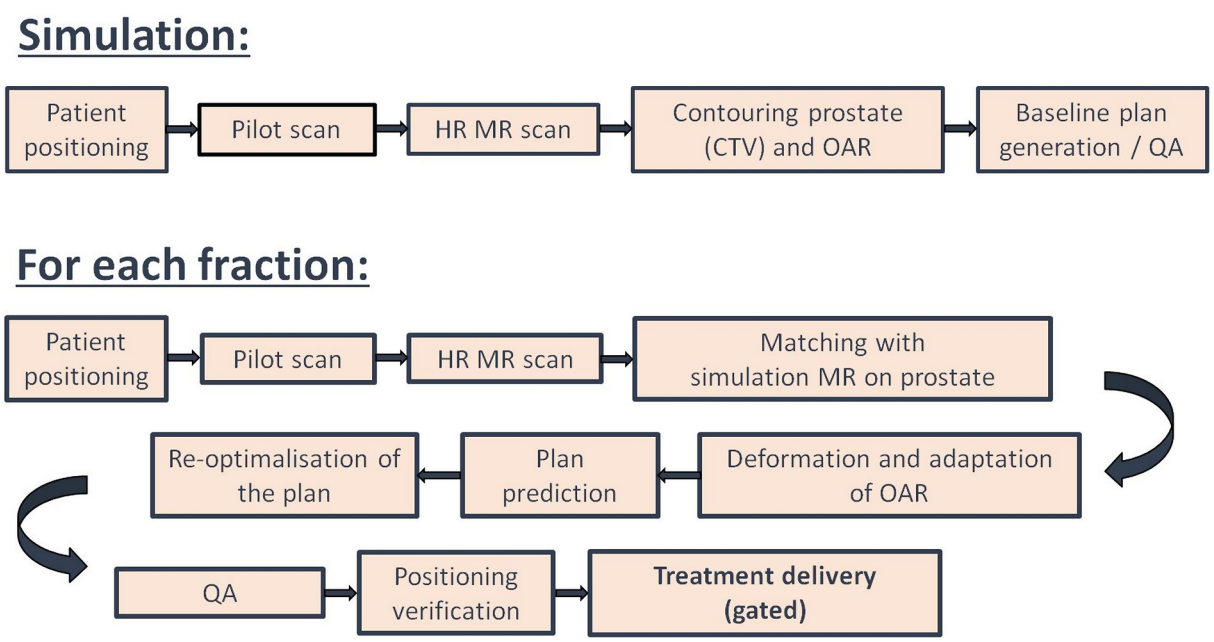

Fig. 2. Workflow for MRgRT with online plan adaptation for prostate cancer. HR = high resolution, MR = magnetic resonance, CTV = clinical target volume, OAR = organs at risk, QA = quality assurance.

questions on potential MR-related complaints and experiences, such as anxiety, temperature, and noise. These items could be scored on a 4-point scale as: “not at all”, “a little”, “moderate”, and “very much”. PRO-Qs were collected once, immediately following the last MRgRT fraction, taking the completion of the PRO-Q on average 5 min.

3. Results

3.1. Target coverage and patient-specific QA

Due to common manual adjustment of the CTV and the 3 mm PTV margin used, the predicted plan is generally suboptimal particularly for target coverage. In 97% (N = 677/700 fractions) of all fractions for prostate MRgRT the plan has been re-optimized. All adapted treatment plans have passed the patient-specific QA and the obtained average γ-pass rate for all 700 adapted fractions is 99.8 ± 0.1%, with $\gamma_{mean} = 0.38 \pm 0.01$.

3.2. Treatment delivery

Beam-on delivery treatment time was on average 10 min and constituted approximately one quarter of the total treatment duration. At the onset of treatment delivery a brief cine movie of 10 s duration was performed at a single sagittal plane (4 frames-per-second, slice thickness 5 mm) previously selected by the physician in order to check the tracking accuracy (Fig. 4). At the same time, it was verified that the position of the CTV had not changed from the first 3D MR-scan at the beginning of the fraction. Gated IMRT delivery was performed using a 3 mm gating boundary around the CTV. The system automatically shut off radiation delivery when the system detected that more than 7% (institute specific setting) of the CTV area is outside of the gating boundary (PTV) during MR-planar acquisition for intra-fraction monitoring. Prostate drifts and intra-fraction prostate rotation/deformation led to application of 2D shifts during treatment delivery in more than 20% of all delivered fractions (149/700 fractions). Larger prostate shifts requiring repeat 3D imaging were observed in approximately 6% of fractions (39/700 fractions).

On average, the duration of an uneventful MRgRT fraction is approximately 45 min (range for all patients, 40–70 min). An overview of the relative duration of all the steps in our MRgRT workflow is shown in Table 1, being recontouring the step which took the longest.

3.3. Patient experiences

The majority of the patients tolerated MRgRT very well, and an overview of most commonly reported complaints is illustrated in Fig. 5. Only a moderate proportion of patients reported light complaints of noise, paresthesia and cold because of the balanced steady-state free precession acquisition during beam-on for intra-fraction monitoring and the relatively long duration of the treatment.

4. Discussion

We have reported on our first clinical experience with MR-guided radiotherapy for prostate cancer patients. While it is customary for prostate cancer radiation therapy to instruct patients to have a full bladder prior to simulation and treatment, this appeared not to be practically for MRgRT. Initiating the MRgRT workflow with full bladder, regularly led to treatment interruptions because of the lengthy delivery time, particularly for later fractions when the first signs of radiation-induced cystitis occur. At present, patients are instructed to empty their bladder two hours before treatment, followed by intake of 500 ml of water. In clinical practice, this usually results in treatment with half full bladder, and variations in bladder and rectal filling can be corrected for by daily plan adaptation. Preselection of patients, based on IPSS scoring is recommended, not only for SBRT in general but certainly also for lengthy MRgRT [32]. Similar as for diagnostic MR scanning, severely claustrophobic patients do not tolerate MRgRT. These patients can be identified at an early stage on the basis of MR safety questionnaires, but in addition, simulation on the MR Linac aids in de-selecting these patients. Once MRgRT was started, no patient discontinued treatment for this reason, although occasional supportive anxiolytic medication was needed [32]. The presence of a hip prosthesis was no absolute contra-indication for MRgRT, as most modern implant materials are MR-compatible, the distortion caused by the metal has proven to be minimal at 0.35 T and, in addition, it has not borne additional difficulties for the delineation of the CTV.

The clinical implementation of (daily adapted) MRgRT constitutes a

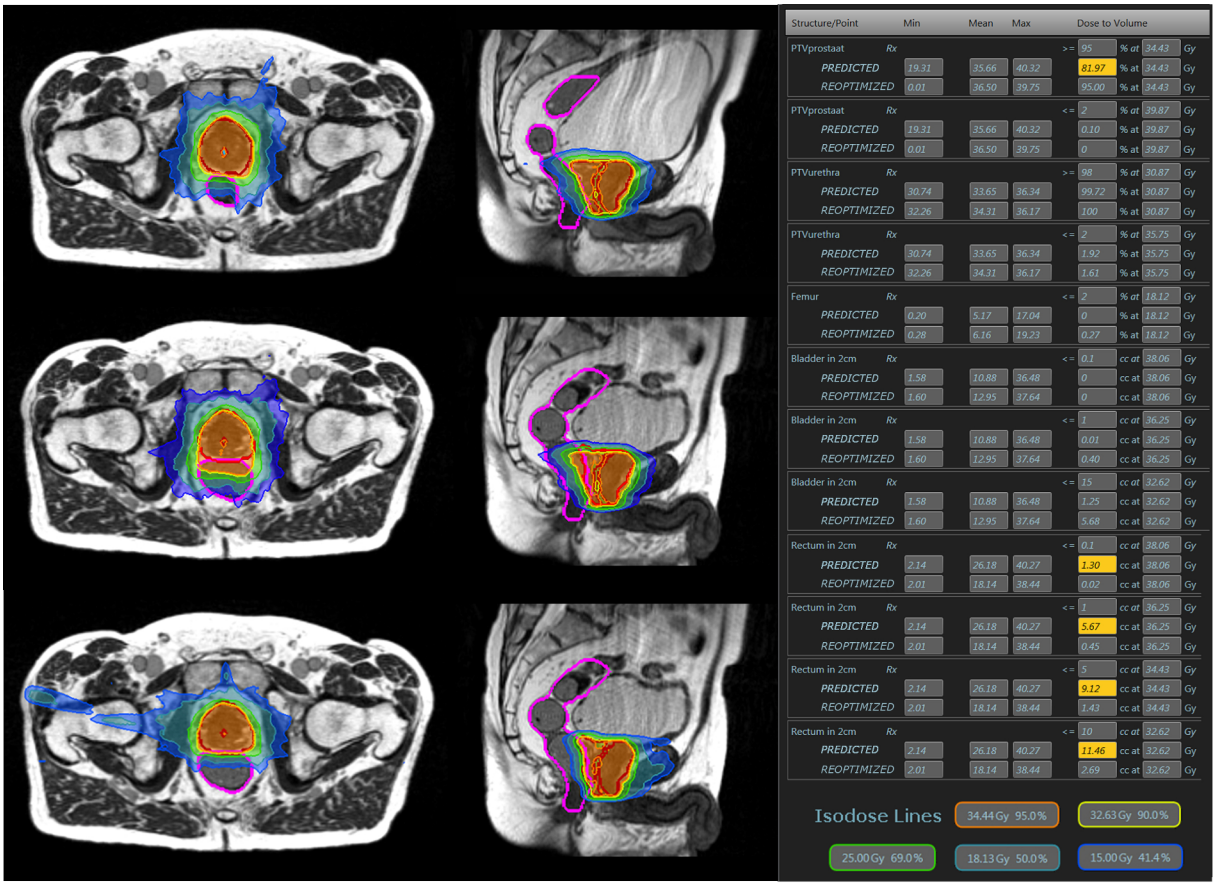

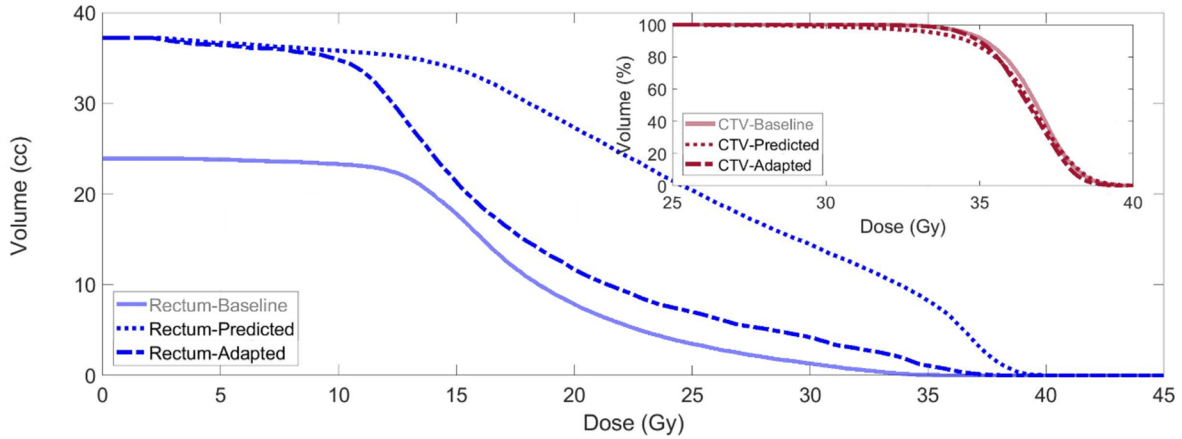

Fig. 3. Treatment plan at baseline (top row), predicted plan (middle row) and adapted plan (bottom row) at one particular fraction. Objectives and clinical constraints according to the institutional protocol for SBRT in prostate cancer can be seen on the right of the figure, where a comparison of the values achieved by the predicted and adapted plan is shown. Values which do not meet the preset values are highlighted in yellow. At the bottom of the figure, a DVH comparison of the three plans is shown. (For interpretation of the references to colour in this figure legend, the reader is referred to the web version of this article.)

major logistic challenge for radiotherapy departments [20,24]. Our MR Linac is used for both simulation and treatment delivery, because using the same MR sequence facilitates subsequent co-registration and delineation. Time slots for treatment are necessarily long (i.e. 45 min up to one hour), which indicates that daily adapted MRgRT is best tailored with (extreme) hypofractionation. We have tried to optimize our workflow by restricting recontouring of relevant OARs to the first 2 cm outside the PTV, which corresponds with the most relevant dose area for clinical toxicity and in which approximately ≥40% of the prescribed dose will be distributed [24,33]. Recontouring full OARs would take an unacceptable long time with the patient in treatment position. Similarly, OAR partitioning and adaptation steps are automatized as much as possible. Importantly, for the recontouring, quality assurance and plan approval steps, a radiation oncologist and physicist need to be physically present at the treatment console for each fraction to avoid further delays. However, even with all this preconditions, an uneventful MRgRT fraction still takes up to 45 min. A significant shorter time for each fraction is possible if further improvement in the deformable registration step of the original contours is achieved. However, other alternatives are also possible for the generation of new contours for both tumor and OARs at each fraction, such as the use of atlas based methods [34] or convolutional neural networks [35,36]. The time spent in recontouring and generating a new treatment plan could also be used to acquire additional MR sequences for offline evaluation of treatment

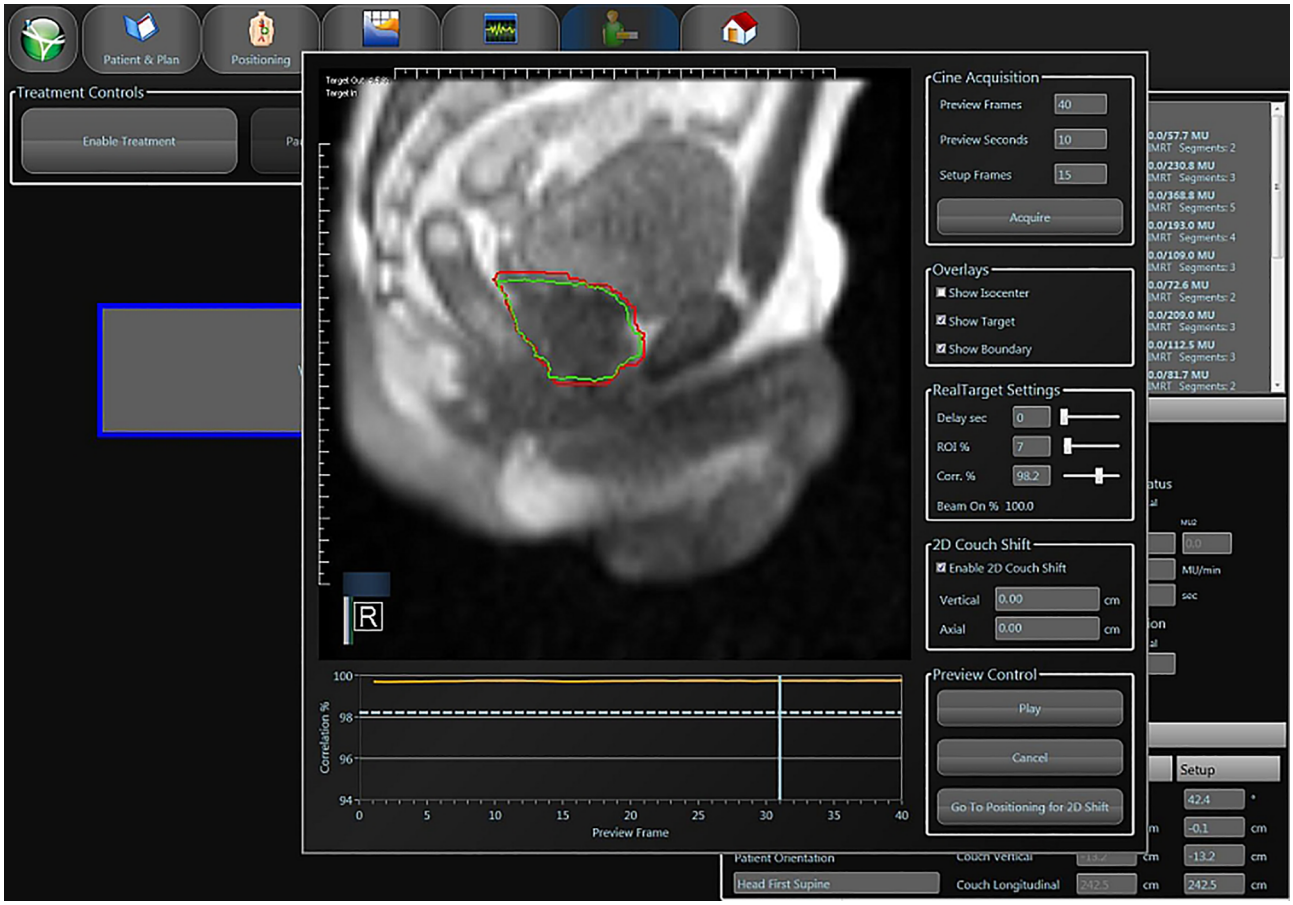

Fig. 4. Gated MRgRT delivery for prostate cancer. The gating target (CTV; green contour) and the gating boundary (red contour) are visualized on-screen. The geometric coverage ("Target out") is continuously displayed in the left upper corner. (For interpretation of the references to colour in this figure legend, the reader is referred to the web version of this article.)

Table 1
Distribution of the measured absolute and relative duration of all steps in daily adapted MRgRT for prostate cancer. The contribution of every discipline to each of the steps is also highlighted on the last three columns (physician, physicist and radiation technologists, from left to right).

SMART step	Time (min)	Physician	Physicist	Therapist
Patient setup	7.6			√
Registration	6.1	√		√
Delineation	10.7	√		√
Re-optimization	2.9	√	√	√
Plan QA	1.5		√	√
Beam-on Tx	15.9	√	√	√
Total	44.7			

response (for instance, diffusion weighted MR [37]).

The ability to perform daily plan adaptation is one key advantage of MRgRT, which appeared to be required in the vast majority of patients. Both residual patient positioning errors and variations in bladder and rectal filling result in the necessity to adjust the contours of the CTV for each fraction, certainly with small 3 mm PTV margins. In actual practice, 97% of plans were delivered after plan re-optimization, mainly for this reason. For an accurate assessment of the predicted dose, i.e. recalculation of the baseline plan on the anatomy of the day, recontouring needs to be performed anyway. The plan adaptation step, including fast independent QA of the generated plan, adds in general just a few minutes to the total treatment duration, as can been seen in Table 1. The dose calculation is performed using the electron density map from the CT-simulation after non-rigid registration to the anatomy of the day. Generation of an electron density map from the MR-scan for that particular fraction is also feasible [38], although this step would not shorten the total treatment session time. Image quality is directly related to a proper placement of the MR coils on the surface of the patient at the region of interest. Accurate patient positioning with the MR coils is also essential because the treatment couch can only be minimally moved in lateral and vertical direction.

The relatively high number of beams being used allows for a conformal dose distribution and offers the necessary degrees of freedom to the optimizer to generate a new fluence map to account for the anatomical changes. In our workflow, a full scope online re-optimization of the fluence and weights for each beam is performed, which usually produces the best results in terms of target coverage and OAR sparing [39]. However, other alternatives have been proposed when optimization and dose calculation time take too long. These include for instance, segment aperture morphing to create new apertures in combination with segment weight optimization [39] and adjustment of MLC leaf position for each subfield based on the inter-fractional target motion and deformation [40].

An innovative feature of MRgRT is the real-time imaging of a sagittal plane through the prostate, bladder and rectum, while visualizing the gating boundary. Prostate drifts have been described previously, one of the reasons why for instance 'triggered imaging' has been introduced into image-guided radiotherapy for prostate cancer. At this moment, real-time guidance with the MRIdian linac is restricted to this single plane. However, it is anticipated that multiplanar MR imaging will be available in the near future, which would result in real 3D tracking of the target volume and improved accuracy. Intra-fractional changes in the prostate position occur relatively frequent, mostly due to

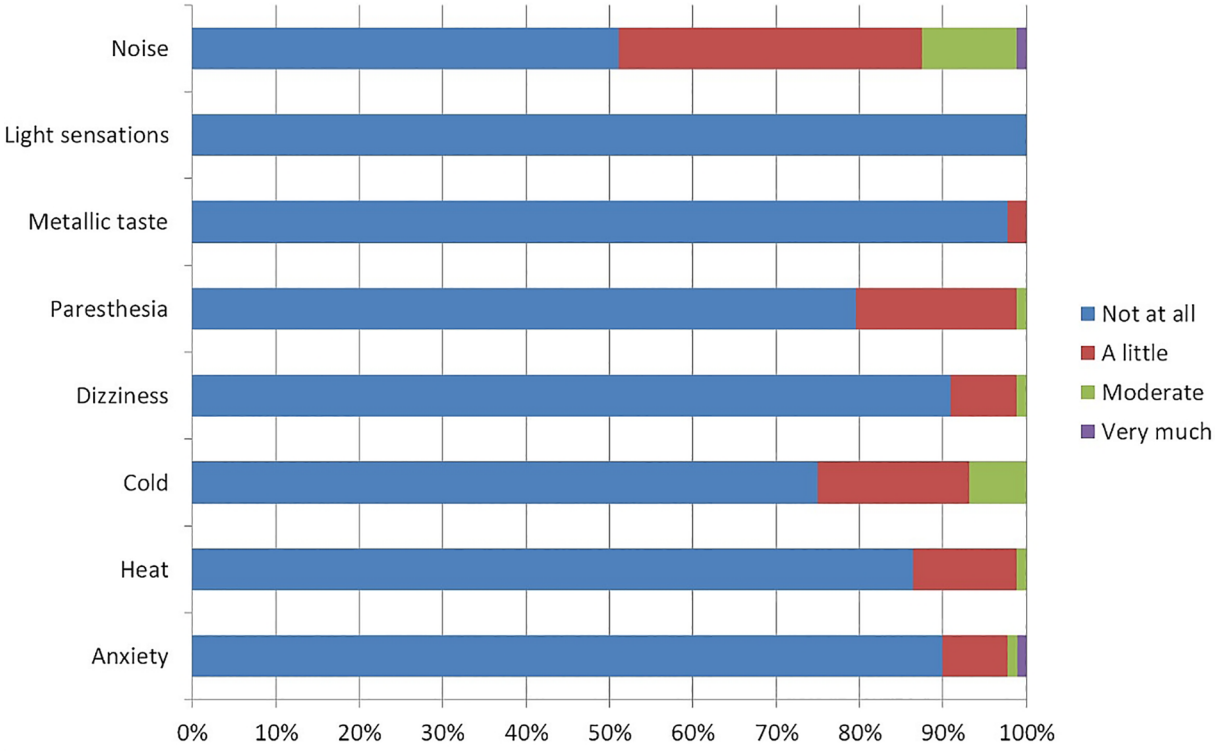

Fig. 5. Patient-reported complaints during MRgRT for prostate cancer (N = 89).

air in the rectum or increasing bladder filling (see also figure in Supplementary material). One relatively simple option to correct for these positional changes is to temporarily interrupt treatment and perform a 2D shift in the table position. This 2D shift, which relies on the anatomical information provided by the MR cine in the sagittal plane, is restricted to the cranio-caudal and/or antero-posterior direction. The system can mechanically perform a shift of several cm, though as an institutional standard we restrict performing 2D shifts to a maximum of 3 mm, which is the PTV margin and also the gating boundary used for tracking. For larger changes in prostate position or suspicions of a lateral movement, treatment is interrupted and 3D positioning scans are repeated, followed by a couch shift correction, recontouring and a new dose prediction when needed. The occurrence of prostate drifts appears not to be uncommon and as a result of 3 mm margins as gating boundary, 2D shifts were needed in more than 20% of all delivered fractions (149/700 fractions). Larger prostate shifts requiring repeat 3D imaging were observed in approximately 6% of fractions (39/700 fractions). In the past it was reported that proper management of intrafractional uncertainty during radiotherapy delivery may allow treatment margin reduction to 3 mm [12]. However, such a small margin makes necessary to introduce refinements to the gated delivery using table adjustments, which has been the major reason for fractions exceeding a total duration of 45 min. At this moment, multiplanar real-time imaging, which would obviously be of benefit, is not yet clinically available on the MRIdian system.

In conclusion, MRgRT as a method to deliver SBRT for prostate cancer has been introduced clinically. This approach is promising but time consuming and logistically challenging requiring a multidisciplinary approach. Because of the advantages of soft-tissue setup without the need for implanted gold markers, online plan adaptation and real-time MR imaging during gated delivery, this technique is expected to expand in the coming years.

Conflict of interest

Ms. Tetar has nothing to disclose. Dr. Bruynzeel reports personal fees from ViewRay Inc., outside the submitted work. Dr. Lagerwaard reports personal fees from ViewRay Inc., outside the submitted work. Prof. Dr. Slotman reports personal fees from ViewRay Inc., outside the submitted work. Mr. Bohoudi has nothing to disclose. Dr. Palacios reports personal fees from ViewRay Inc., outside the submitted work.

Appendix A. Supplementary data

Supplementary data to this article can be found online at https://doi.org/10.1016/j.phro.2019.02.002.

References

[1] Jz W, Guerrero M, Allen Li X. How low is the α/β ratio for prostate cancer? Int J Radiat Oncol Biol Phys 2003;57:1116–21. https://doi.org/10.1016/S0360-3016(03)01455-X.
[2] Miralbell R, Roberts SA, Zubizarreta E, Hendry JH. Dose-fractionation sensitivity of prostate cancer deduced from radiotherapy outcomes of 5,969 patients in seven international institutional datasets: α/β = 1.4 (0.9-2.2) Gy. Int J Radiat Oncol Biol Phys 2012;82:17–24. https://doi.org/10.1016/j.ijrobp.2010.10.075.
[3] Proust-Lima C, Taylor JMG, Sécher S, Sandler H, Kestin L, Pickles T, et al. Confirmation of a low α/β ratio for prostate cancer treated by external beam radiation therapy alone using a post-treatment repeated-measures model for PSA dynamics. Int J Radiat Oncol Biol Phys 2011;79:195–201. https://doi.org/10.1016/j.ijrobp.2009.10.008.
[4] Pinkawa M, Siluschek J, Gagel B, Demirel C, Asadpour B, Holy R, et al. Influence of the initial rectal distension on posterior margins in primary and postoperative radiotherapy for prostate cancer. Radiother Oncol 2006;81:284–90. https://doi.org/10.1016/j.radonc.2006.10.028.
[5] Pinkawa M, Asadpour B, Siluschek J, Gagel B, Piroth MD, Demirel C, et al. Bladder extension variability during pelvic external beam radiotherapy with a full or empty bladder. Radiother Oncol 2007;83:163–7. https://doi.org/10.1016/j.radonc.2007.03.015.
[6] Landoni V, Saracino B, Marzi S, Gallucci M, Petrongari MG, Chianese E, et al. A study of the effect of setup errors and organ motion on prostate cancer treatment with IMRT. Int J Radiat Oncol Biol Phys 2006;65:587–94. https://doi.org/10.1016/j.ijrobp.2006.01.021.
[7] De Crevoisier R, Tucker SL, Dong L, Mohan R, Cheung R, Cox JD, et al. Increased risk of biochemical and local failure in patients with distended rectum on the planning CT for prostate cancer radiotherapy. Int J Radiat Oncol Biol Phys 2005;62:965–73. https://doi.org/10.1016/j.ijrobp.2004.11.032.
[8] McPartlin AJ, Li XA, Kershaw LE, Heide U, Kerkmeijer L, Lawton C, et al. MRI-guided prostate adaptive radiotherapy – a systematic review. Radiother Oncol 2016.

https://doi.org/10.1016/j.radonc.2016.04.014.
[9] Moteabbed M, Trofimov A, Khan FH, Wang Y, Sharp GC, Zietman AL, et al. Impact of interfractional motion on hypofractionated pencil beam scanning proton therapy and VMAT delivery for prostate cancer. Med Phys 2018;45:4011–9. https://doi.org/10.1002/mp.13091.
[10] Sheng Y, Li T, Lee WR, Yin FF, Wu QJ. Exploring the margin recipe for online adaptive radiation therapy for intermediate-risk prostate cancer: an intrafractional seminal vesicles motion analysis. Int J Radiat Oncol Biol Phys 2017;98:473–80. https://doi.org/10.1016/j.ijrobp.2017.02.089.
[11] Tanyi JA, He T, Summers PA, Mburu RG, Kato CM, Rhodes SM, et al. Assessment of planning target volume margins for intensity-modulated radiotherapy of the prostate gland: Role of daily inter- and intrafraction motion. Int J Radiat Oncol Biol Phys 2010;78:1579–85. https://doi.org/10.1016/j.ijrobp.2010.02.001.
[12] Deutschmann H, Kametriser G, Steininger P, Scherer P, Schöller H, Gaisberger C, et al. First clinical release of an online, adaptive, aperture-based image-guided radiotherapy strategy in intensity-modulated radiotherapy to correct for inter- and intrafractional rotations of the prostate. Int J Radiat Oncol Biol Phys 2012;83:1624–32. https://doi.org/10.1016/j.ijrobp.2011.10.009.
[13] Peng C, Ahunbay E, Chen G, Anderson S, Lawton C, Li XA. Characterizing interfraction variations and their dosimetric effects in prostate cancer radiotherapy. Int J Radiat Oncol Biol Phys 2011;79:909–14. https://doi.org/10.1016/j.ijrobp.2010.05.008.
[14] Ahunbay EE, Li XA. Gradient maintenance: a new algorithm for fast online replanning a). Med Phys 2015;42:2863–76. https://doi.org/10.1118/1.4919847.
[15] McVicar N, Popescu IA, Heath E. Techniques for adaptive prostate radiotherapy. Phys Medica 2016;32:492–8. https://doi.org/10.1016/j.ejmp.2016.03.010.
[16] Kashani R, Olsen JR. Magnetic resonance imaging for target delineation and daily treatment modification. Semin Radiat Oncol 2018;28:178–84. https://doi.org/10.1016/j.semradonc.2018.02.002.
[17] Palacios MA, Bohoudi O, Bruynzeel AME, van Sörnsen-de Koste JR, Cobussen P, Slotman BJ, et al. Role of daily plan adaptation in MR-guided stereotactic ablative radiotherapy for adrenal metastases. Int J Radiat Oncol 2018. https://doi.org/10.1016/j.ijrobp.2018.06.002.
[18] Henke L, Kashani R, Yang D, Zhao T, Green O, Olsen L, et al. Simulated online adaptive magnetic resonance-guided stereotactic body radiation therapy for the treatment of oligometastatic disease of the abdomen and central thorax: characterization of potential advantages. Int J Radiat Oncol Biol Phys 2016;96:1078–86. https://doi.org/10.1016/j.ijrobp.2016.08.036.
[19] Raaymakers BW, Jürgenliemk-Schulz IM, Bol GH, Glitzner M, Kotte ANTJ, Van Asselen B, et al. First patients treated with a 1.5 T MRI-Linac: clinical proof of concept of a high-precision, high-field MRI guided radiotherapy treatment. Phys Med Biol 2017;62:L41–50. https://doi.org/10.1088/1361-6560/aa9517.
[20] Pathmanathan AU, van As NJ, Kerkmeijer LGW, Christodouleas J, Lawton CAF, Vesprini D, et al. Magnetic resonance imaging-guided adaptive radiation therapy: a "game changer" for prostate treatment? Int J Radiat Oncol Biol Phys 2018;100:361–73. https://doi.org/10.1016/j.ijrobp.2017.10.020.
[21] Salembier C, Villeirs G, De Bari B, Hoskin P, Pieters BR, Van Vulpen M, et al. ESTRO ACROP consensus guideline on CT- and MRI-based target volume delineation for primary radiation therapy of localized prostate cancer. Radiother Oncol 2018;127:49–61. https://doi.org/10.1016/j.radonc.2018.01.014.
[22] Heidenreich A, Bastian PJ, Bellmunt J, Bolla M, Joniau S, Van Der Kwast T, et al. EAU guidelines on prostate cancer. Part 1: screening, diagnosis, and local treatment with curative intent – update 2013. Eur Urol 2014;65:124–37. https://doi.org/10.1016/j.eururo.2013.09.046.
[23] Bohoudi O, Palacios MA, Slotman BJ, Senan S, Bruynzeel AME, Lagerwaard FJ. OC-0519: radiotherapy plan quality using a double focused, double stacked multi-leaf collimator. Radiother Oncol 2018;127:S273. https://doi.org/10.1016/S0167-8140(18)30829-6.
[24] Bohoudi O, Bruynzeel AME, Senan S, Cuijpers JP, Slotman BJ, Lagerwaard FJ, et al. Fast and robust online adaptive planning in stereotactic MR-guided adaptive radiation therapy (SMART) for pancreatic cancer. Radiother Oncol 2017;125:439–44. https://doi.org/10.1016/j.radonc.2017.07.028.
[25] Kawrakow I, Fippel M. Investigation of variance reduction techniques for Monte Carlo photon dose calculation using XVMC. Phys Med Biol 2000;45:2163–84.
[26] Kawrakow I. Accurate condensed history Monte Carlo simulation of electron transport. I. EGSnrc, the new EGS4 version. Med Phys 2000;27:485–98. https://doi.org/10.1118/1.598917.
[27] Palacios MA, Apicella T, Hoffmans D, Osario TR, Admiraal M, Kawrakow I, et al. Implementation of patient specific QA for daily adaptive MR-guided radiation therapy. Radiother Oncol 2017;123:S134–5. https://doi.org/10.1016/S0167-8140(17)30705-3.
[28] Li HH, Rodriguez VL, Green OL, Hu Y, Kashani R, Wooten HO, et al. Quality assurance for the delivery of 60Co intensity modulated radiation therapy subject to a 0.35-T lateral magnetic field. Int J Radiat Oncol 2015;91:65–72. https://doi.org/10.1016/j.ijrobp.2014.09.008.
[29] Low DA, Dempsey JF. Evaluation of the gamma dose distribution comparison method. Med Phys 2003;30:2455. https://doi.org/10.1118/1.1598711.
[30] Low DA, Harms WB, Mutic S, Purdy JA. A technique for the quantitative evaluation of dose distributions. Med Phys 1998:656–61.
[31] Sempau J, Wilderman S, Bielajew A. DPM, a fast, accurate Monte Carlo code optimized for photon and electron radiotherapy treatment planning dose calculations. Phys Med Biol 2000;45:2263–92.
[32] Tetar S, Bruynzeel A, Bakker R, Jeulink M, Slotman BJ, Oei S, et al. Outcome measurements on the tolerance of magnetic resonance. Imag-guided Radiat Ther Cureus 2018;10. https://doi.org/10.7759/cureus.2236.
[33] Lamb J, Cao M, Kishan A, Agazaryan N, Thomas DH, Shaverdian N, et al. Adaptive radiation therapy: implementation of a new process of care. Cureus 2017;9. https://doi.org/10.7759/cureus.1618.
[34] Lustberg T, van Soest J, Gooding M, Peressutti D, Aljabar P, van der Stoep J, et al. Clinical evaluation of atlas and deep learning based automatic contouring for lung cancer. Radiother Oncol 2017;126:312–7. https://doi.org/10.1016/j.radonc.2017.11.012.
[35] Men K, Zhang T, Chen X, Chen B, Tang Y, Wang S, et al. Fully automatic and robust segmentation of the clinical target volume for radiotherapy of breast cancer using big data and deep learning. Phys Med 2018;50:13–9. https://doi.org/10.1016/j.ejmp.2018.05.006.
[36] Feng M, Valdes G, Dixit N, Solberg TD. Machine learning in radiation oncology: opportunities, requirements, and needs. Front Oncol 2018;8:1–7. https://doi.org/10.3389/fonc.2018.00110.
[37] Liu F, Erickson B, Peng C, Li XA. Characterization and management of interfractional anatomic changes for pancreatic cancer radiotherapy. Int J Radiat Oncol Biol Phys 2012;83:e423–9. https://doi.org/10.1016/j.ijrobp.2011.12.073.
[38] Owrangi AM, Greer PB, Glide-Hurst CK. MRI-only treatment planning: benefits and challenges. Phys Med Biol 2018;63:1–15. https://doi.org/10.1088/1361-6560/aaaca4.
[39] Ahunbay EE, Peng C, Chen GP, Narayanan S, Yu C, Lawton C, et al. An on-line replanning scheme for interfractional variations. Med Phys 2008;35:3607–15. https://doi.org/10.1118/1.2952443.
[40] Fu W, Yang Y, Yue N, Heron D, Huq M. A Cone Beam CT—guided online plan modification technique to correct interfractional anatomic changes for prostate cancer IMRT treatment. Med Phys 2007;34:2368. https://doi.org/10.1118/1.2760507.